SOILS AND FOUNDATIONS Vol. 48, No. 6, 821–831, Dec. 2008
Japanese Geotechnical Society

FORMULATION OF G_{max} FROM RECONSTITUTED CLAYEY SOILS AND ITS APPLICATION TO G_{max} MEASURED IN THE FIELD

TAKAYUKI KAWAGUCHI[i] and HIROYUKI TANAKA[ii]

ABSTRACT

The elastic shear modulus of natural sedimentary clay ground, G_{max}, is estimated based on laboratory tests for fifteen different reconstituted clays. Two types of tests were performed, i.e., Bender Element and Cyclic Triaxial tests. The proposed formulation is not based on void ratio, e, but consists of only three parameters: w_L (liquid limit), p' (the current mean effective stress) and p'_{max} (the maximum mean consolidation pressure). To apply it to the field, this equation is modified for using σ'_{v0} (the in situ effective overburden pressure) and OCR, instead of p' and p'_{max}. Since existing formulae for G_{max} are mostly based on e, they are not able to apply to both reconstituted soil and field, without considering the correction factor for structure. This is because e in the field is much larger than that for reconstituted soil even though their consolidation pressures and OCR are the same for these clays. The applicability of the proposed formula was examined by using investigated results from the in-situ seismic surveys performed at eleven worldwide sites. It is well demonstrated that the proposed equation in this paper is capable of predicting G_{max} of natural sedimentary clay deposits with higher accuracy than the existing empirical formulae using a function of e.

Key words: clay, in-situ test, laboratory test, shear modulus, small strain (**IGC**: D6/D7)

INTRODUCTION

Geomaterials exhibit quasi-elastic behavior at small strains less than 10^{-6}. The maximum elastic shear modulus G_{max} as well as the elastic Young's modulus E_{max}, which may be observed in these small strain levels, is a very important soil property for seismic response analysis in practice. These elastic properties are able to be measured by in-situ seismic surveys (e.g., seismic cone test, PS-logging and so on) and also from laboratory testing such as triaxial, torsional shear and bender element tests. However, these seismic tests either in the field or at laboratory are rarely carried out in routine investigations. Instead, G_{max} or E_{max} is usually estimated by empirical relations or equations, using fundamental properties, such as void ratio, e or confining stresses.

As will be mentioned in more detail, empirical equations for estimating G_{max} or E_{max} are usually based on void ratio, e, as shown in Eq. (1).

$$G_{max} = A \cdot f(e) \cdot \left(\frac{p'}{p'_r}\right)^n \cdot (\mathrm{OCR})^k \tag{1}$$

where A is a constant having the same dimension as G_{max}, $f(e)$ is a function of e, OCR is over-consolidation ratio, p' is the mean effective stress and normalized by a reference pressure of p'_r, and n and k are both experimental exponents. The value of exponent n is usually around 0.5 (e.g., Hardin and Black, 1969; Marcuson and Wahls, 1972; Zen et al., 1978).

A reason for using e may be attributed to historical facts that researches on G_{max} started with sandy soils. Properties of sandy soils are strongly affected by e and change in e caused by p' changing is relatively small. It may be reasonable that G_{max} is correlated separately to p' and e for sandy soils. For clayey soils, however, e decreases with increase in p', especially at normally consolidated (NC) state: i.e., $f(e)$ in Eq. (1) is also function of p'. Furthermore, Jamiolkowski et al. (1994) have demonstrated that if a proper $f(e)$ is selected, then G_{max} seems not to be influenced by OCR and depends only on the current p' ($k=0$).

Due to repeatability of test results and an economical reason for tested specimens, fundamental geotechnical parameters including G_{max} and E_{max} have been studied using reconstituted soils. However, the most significant difference in geotechnical properties between reconstituted and intact samples is the order of e, i.e.: even in conditions with the same p' and OCR as the in-situ, e for intact soils is significantly greater than that for reconstituted soils, even though intact samples are experienced by long term of secondary consolidation (for example, Tanaka, et al., 2004). This difference is explained by many researchers in terms of structure or cementation, which are developed during the long term deposition process. In this

[i] Associate Professor, Department of Civil Engineering, Hakodate National College of Technology, Japan (kawa@hakodate-ct.ac.jp).
[ii] Associate Professor, Division of Solid Waste, Resources and Geoenvironmental Engineering, Graduate School of Engineering, Hokkaido University, Japan.
The manuscript for this paper was received for review on March 17, 2008; approved on October 10, 2008.
Written discussions on this paper should be submitted before July 1, 2009 to the Japanese Geotechnical Society, 4-38-2, Sengoku, Bunkyo-ku, Tokyo 112-0011, Japan. Upon request the closing date may be extended one month.

reason, soil parameters required for estimating the in situ G_{max}, A, $f(e)$ and n (if necessary, k) in Eq. (1) are obtained from field data, not from data measured by laboratory tests for reconstituted soils (for example, Shibuya and Tanaka, 1996).

In this paper, we propose a new equation for G_{max}, based on test results from reconstituted soils without the aid of $f(e)$, as shown in Eq. (2).

$$G_{max} = 20000 \cdot w_L^{-0.8} \cdot p'^{0.6} \cdot p'^{0.2}_{max} \tag{2}$$

where, w_L is liquid limit (in percent). p' and p'_{max} (in kPa) are the mean effective stresses at measurement of G_{max} (in kPa) and the maximum mean effective stresses, respectively.

The most distinguished point in Eq. (2) compared with existing equations (i.e., Eq. (1)) is that this equation is not related to e. This paper will describe the process for deriving Eq. (2) from a lot of data measured by reconstituted samples. In addition, applicability of Eq. (2) to the field will be examined. There is a difficulty in the form of Eq. (2) to apply directly to the field, because Eq. (2) requires the horizontal effective stress, σ'_h, for calculating p' and p'_{max}. Therefore, finally Eq. (3) is proposed to estimate G_{max} measured by seismic survey in the field.

$$G_{max} = 20000 \cdot w_L^{-0.8} \cdot f(\mathrm{OCR}) \cdot \sigma'^{0.8}_{v0} \tag{3}$$

where, σ'_{v0} is the in-situ effective overburden pressure; $f(\mathrm{OCR})$ is the function required for converting p' to σ'_v and can be expressed by Eq. (4).

$$f(\mathrm{OCR}) = \left(\frac{2}{3}\mathrm{OCR}\right)^{0.2} \cdot \left(\frac{1+\mathrm{OCR}^{0.5}}{3}\right)^{0.6} \tag{4}$$

In the later part of this paper, applicability of Eq. (4) will be examined using the field data base accumulated by the authors.

TESTING METHODS

Laboratory Tests for Using Reconstituted Samples

Table 1 shows the summary of fundamental properties of reconstituted clay samples, together with parameters required for formulating G_{max} proposed in this study. Samples were constituted to be consolidated from slurry state with initial water content two times larger than liquid limit, w_L. Two clays, i.e., NSF clay and MC clay, are commercially available as powder, and the other clays were prepared from natural clay samples. Figure 1 shows index properties of tested clays in the plasticity chart. It is recognized that these clays have large varieties in index properties.

Elastic properties at small strains were measured by shear wave velocity using bender element and by cyclic/monotonic loading in triaxial tests. G_{max} at Normally Consolidated (NC) and OverConsolidated (OC) states was measured in an oedometer ring attaching a pair of bender elements (denoted by OEBE in Table 1), where G_{max} corresponds to G_{vh} that is associated with the grain motion in the horizontal direction with shear wave propagating in the vertical direction. The specimen in the oedometer ring is 60 mm in diameter and 20 mm in initial height. The horizontal stress was measured by strain gauges glued on the oedometer ring so that p' can be calculated at measurement of G_{vh} (Shibuya et al., 1997). The travel time for G_{vh} by the Bender Element was defined as ''start-to-start'' of the generated and arriving waves (Kawaguchi et al., 2001).

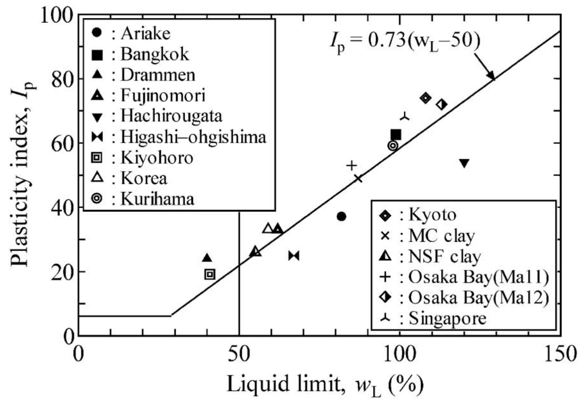

Fig. 1. Reconstituted clays in the plasticity chart

The undrained elastic Young's modulus, $(E_v)_u$, at small strains was measured in triaxial apparatus (TX in Table 1) equipped with a direct drive motor (Shibuya and Mitachi, 1997). In this apparatus, a specimen with the dimension of 50 mm in diameter and 100 mm in height was subjected to cyclic/monotonic stresses at an axial strain amplitude of about 0.001% (10^{-5}). The axial deformation was measured by counting the rotation of the direct drive motor (Kawaguchi et al., 2002). In addition, a new version TX equipped with a pair of bender elements, TXBE, was used for simultaneous measurement of $(E_v)_u$ and G_{vh} (Kawaguchi et al., 2003).

Correlation between $(E_v)_u$ and G_{vh}

As indicated in Table 1, elastic moduli are measured by OEBE and TX apparatus. From OEBE, the measured elastic modulus is G_{vh} obtained, while $(E_v)_u$ is measured by TX. Therefore, it is required to make a correlation between G_{vh} and $(E_v)_u$. It is reported that elastic modulus of geomaterials exhibits cross-anisotropy behavior (for example, Atkinson, 1975; Bishop and Hight, 1977; Graham and Houlsby, 1983). In such a material, the conventional relation of $E = G/3$ cannot be used for evaluation of elastic modulus.

Figure 2 shows relations between $(E_v)_u/3G_{vh}$ and G_{hh}/G_{vh} is calculated using the micro-mechanics model proposed by Yimsiri and Soga (2002, 2003). In the figure, G_{hh} is the elastic shear modulus corresponding to the state that both the grain motion and propagation of the shear wave are in the horizontal direction. K_R and K_N indicate tangential and normal rigidity at contacts of soil grains, respectively. It can be seen in Fig. 2 that the ratio of $(E_v)_u$ to $3G_{vh}$ lies within 10% difference when G_{hh}/G_{vh} ranges between 0.8 and 2.0. This calculation result demonstrates that an effect of cross anisotropy is small enough to assume to use Eq. (5) for evaluation of elastic modulus in

Table 1. Properties of fifteen reconstituted clays examined in this study

	Apparatus	w_L (%)	IP	λ	κ	N	ψ	ξ	Z	References
Ariake	OEBE	82.0	37.0	0.255	0.0686	2.889	0.283	0.0858	5.007	Shibuya et al. (1997)
Bangkok	OEBE	98.7	62.6	0.312	0.0270	2.921	0.388	0.0402	5.736	Hwang (1998)
Drammen	OEBE	40.0	24.0	0.102	0.0203	1.301	0.133	0.0235	2.391	Shibuya et al. (1997)
Fujinomori	TX	62.0	33.0	0.207	0.0385	2.420	0.273	0.0796	4.471	This study
Hachirougata	OEBE	120.0	54.0	0.285	0.0743	2.841	0.332	0.0970	5.313	Shibuya et al. (1997)
Higashi-Ohgishima	OEBE	67.0	25.0	0.191	0.0246	2.186	0.239	0.0468	4.038	Shibuya et al. (1997)
Kiyohoro	OEBE	41.0	19.0	0.090	0.0177	1.137	0.142	0.0276	2.420	Shibuya et al. (1997)
Pusan	TX	59.0	33.1	0.138	0.0295	1.817	0.185	0.0527	3.239	Li (2003)
Kurihama	OEBE	98.0	59.0	0.296	0.0460	3.071	0.354	0.1052	5.646	Shibuya et al. (1997)
Kyoto	TXBE	108.0	74.0	0.344	0.0635	3.407	0.448	0.1004	6.604	Li (2003)
MC clay	OEBE	87.0	49.0	0.270	0.0750	2.928	0.401	0.1271	5.986	Shibuya et al. (1997)
NSF clay	TX, TXBE	55.0	26.0	0.141	0.0285	1.945	0.193	0.0572	3.470	This study
Osaka Bay (Ma11)	TXBE	85.0	53.0	0.379	0.0671	3.862	0.460	0.1127	7.014	Li (2003)
Osaka Bay (Ma12)	TXBE	113.0	72.0	0.282	0.0571	2.911	0.347	0.1073	5.358	Li (2003)
Singapore	TX	101.5	68.1	0.227	0.0570	2.465	0.276	0.1000	4.304	Li (2003)

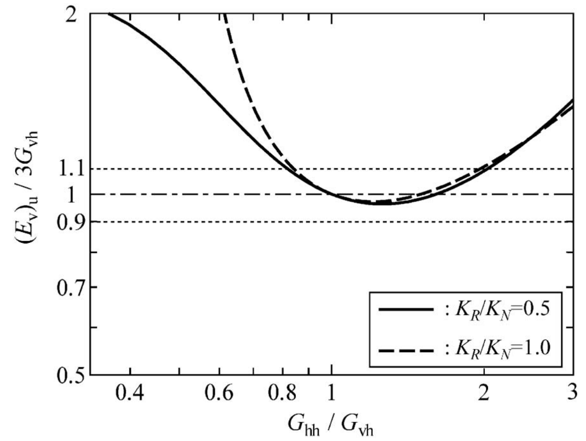

Fig. 2. Relationship between $(E_v)_u/3G_{vh}$ and G_{hh}/G_{vh} calculated following micro-mechanics model proposed by Yimsiri and Soga (2002, 2003)

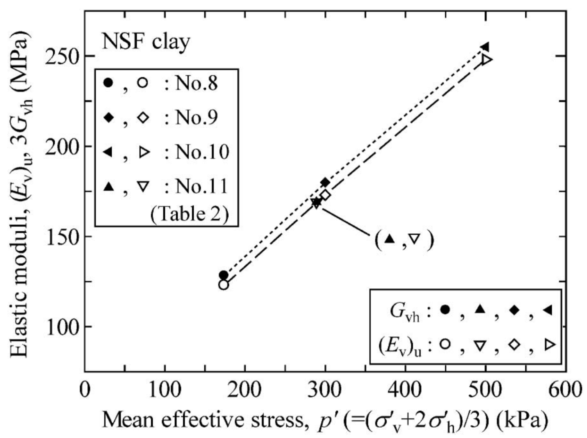

Fig. 3. Comparisons of $(E_v)_u$ with $3G_{vh}$ (Test No. *see* Table 2)

this range.

$$(E_v)_u = 3G_{vh} \tag{5}$$

Figure 3 shows the comparison between $(E_v)_u$ and $3G_{vh}$ measured by laboratory test for NSF clay. The test conditions in Test No. in the legend of the figure are described in Table 2. Note that $(E_v)_u$ was determined by fitting a linearity between deviator stress and axial strain for a small strain range less than 0.005%. As can be seen in Fig. 3, $(E_v)_u$ is more or less equal to 3 G_{vh}. In addition, there are experimental evidences showing that the ratio of G_{hh}/G_{vh} is about 1.0–1.8 for NSF clay (Kawaguchi et al., 2007) and for other soft clays the G_{hh}/G_{vh} ratio ranges roughly between 1.0 and 2.0 (e.g., Jovičić and Coop, 1995; Ling et al., 2000; Yamashita and Suzuki, 2001; Yimsiri and Soga, 2002, 2003). Therefore, it may be concluded that Eq. (5) is applicable to most soft clays. In this study, $(E_v)_u$ measured by the TX test can be converted to G_{vh} by using Eq. (5) and compared to G_{vh} from the OEBE test.

Seismic Surveys for Natural Clay Deposits

Table 3 shows geotechnical properties at 11 sites where seismic survey was performed. As examples, G_{max} profiles measured at Ariake and Pusan sites are shown in Fig. 4, where other properties obtained at relevant boreholes such as over-consolidation ratio, OCR ($=\sigma'_{vy}/\sigma'_{v0}$, where σ'_{vy} is the yield consolidation stress measured by Constant Rate of Strain (CRS) oedometer test with a strain rate of 0.02%/min), natural water content, w_n, and index properties are also plotted. Clay samples were retrieved by the Japanese Standard fixed piston thin wall sampler. Shear

Table 2. Conditions and some results of tests performed on NSF clay

Test No.	K-value*	OCR (p'_{max}/p')	$p'^{§}$	$\sigma'^{§}_{v}$	Condition of shearing	Elastic moduli (MPa)
1	1.0	1	278	279	Cyclic	$(E_v)_u=168$
2	0.8	1	242	279	Cyclic	$(E_v)_u=153$
3	1.0	1	202	202	Monotonic	$(E_v)_u=137$
4	0.6	1	204	277	Monotonic	$(E_v)_u=139$
5	1.0	1	302	302	Monotonic	$(E_v)_u=180$
6	1.0	4	77	78	Monotonic	$(E_v)_u=80$
7	1.0	8	40	40	Monotonic	$(E_v)_u=54$
8	1.0	1	174	174	Monotonic & BE	$(E_v)_u=123$, $G_{vh}=43$
9	1.0	1	300	300	Monotonic & BE	$(E_v)_u=173$, $G_{vh}=60$
10	1.0	1	500	500	Monotonic & BE	$(E_v)_u=248$, $G_{vh}=85$
11	K_0 (0.59)	1	289	400	Monotonic & BE	$(E_v)_u=169$, $G_{vh}=56$
12	1.0	1	175→299→400→500	175→299→400→499	Monotonic & BE	$(E_v)_u=131\rightarrow184\rightarrow229\rightarrow262$ $G_{vh}=45\rightarrow64\rightarrow78\rightarrow91$
13	1.0	1, 2, 6	161→220→300→161→50	161→220→300→161→50	Cyclic	$(E_v)_u=114\rightarrow142\rightarrow168\rightarrow128\rightarrow67$
14	0.6	1, 2, 6	161→220→300→161→50	220→300→409→220→68	Cyclic	$(E_v)_u=111\rightarrow139\rightarrow167\rightarrow124\rightarrow65$

*: under consolidation/swelling, §: at measuring elastic deformation moduli

Table 3. Properties and results of in situ seismic surveys at eleven sites worldwide

	Origin	Depth (m)	w_L (%)	IP	OCR	G_f (MPa)	Reference
Ariake	Japan	3.5–17.5	66.6–128.3	35.3–81.3	1.13–2.17	3.0–20.0	Tanaka et al. (2001a)
Amagasaki	Japan	11.4–19.4	75.0–104.0	47.9–69.1	1.37–2.44	24.4–60.0	Temma et al. (2000)
Bangkok	Thailand	5.8–14.5	45.8–97.3	26.4–63.1	1.17–1.78	9.7–26.0	Tanaka et al. (2001a)
Bothkennar	U.K.	2.8–16.1	55.2–76.9	32.6–45.6	2.19–3.55	11.2–36.9	Nash et al. (1992)
Hachirougata	Japan	3.0–23.0	123.8–238.8	76.6–150.2	0.87–1.94	1.2–12.6	Tanaka (2006)
Izumo	Japan	9.0–28.0	75.4–152.3	26.1–106.5	0.88–1.08	7.2–16.6	Shibuya and Tanaka (1996)
Louiseville	Canada	2.0–10.5	64.0–73.0	39.0–47.0	2.02–2.93	15.0–28.0	Tanaka et al. (2001b)
Osaka Bay	Japan	276.0–389.0	39.0–120.2	17.6–82.7	1.4 (assumed)	198.0–504.0	Tanaka et al. (2002)
Pusan	Korea	5.8–21.8	53.0–72.9	30.8–47.0	1.06–2.92	13.8–31.5	Tanaka et al. (2001c)
Singapore	Singapore	14.5–27.5	50.2–82.3	33.9–57.7	1.06–1.73	30.0–48.0	Tanaka et al. (2001a)
Yamashita Park	Japan	20.5–35.5	92.5–123.6	54.5–76.3	1.67–2.42	40.2–62.6	Tanaka et al. (2001b)

wave velocity, v_s, was measured by a down-hole type of the seismic cone (Tanaka et al., 1994), except for Osaka Bay where a suspension method was employed because of great depth. Figure 5 shows a plasticity chart of the natural clays tested in this study. Data for Bothkennar are referred to Nash et al. (1992) and for Louiseville were obtained from the Laval Geotechnical group.

ELASTIC MODULUS FOR RECONSTITUTED CLAYS

Influence of Anisotropical Consolidation

Using NSF clay, $(E_v)_u$ was measured under various conditions as indicated in Table 2. In order to investigate the effects of anisotropical consolidation pressures on the $(E_v)_u$ value, a pair of TX tests with different stress paths was conducted, i.e., tests No. 13 and No. 14 in Table 2. The specimen for test No. 13 was isotropically consolidated, while the specimen for test No. 14 was consolidated under $K=0.6$ ($K=\sigma'_h/\sigma'_v$, where σ'_h and σ'_v are horizontal and vertical effective stresses, respectively). Their stress paths are indicated in Fig. 6(a). It can be seen in Fig. 6(b) that the values of $(E_v)_u$ at the same σ'_v are different, while the values of $(E_v)_u$ at the same p' are almost identical. Also, it should be noted that e–log p' relations for $K=1.0$ and 0.6 are nearly the same (*see* in Fig. 6(c)). It may be concluded from these relations that the values of $(E_v)_u$ (or G_{vh}) can be expressed in terms of p' alone, and

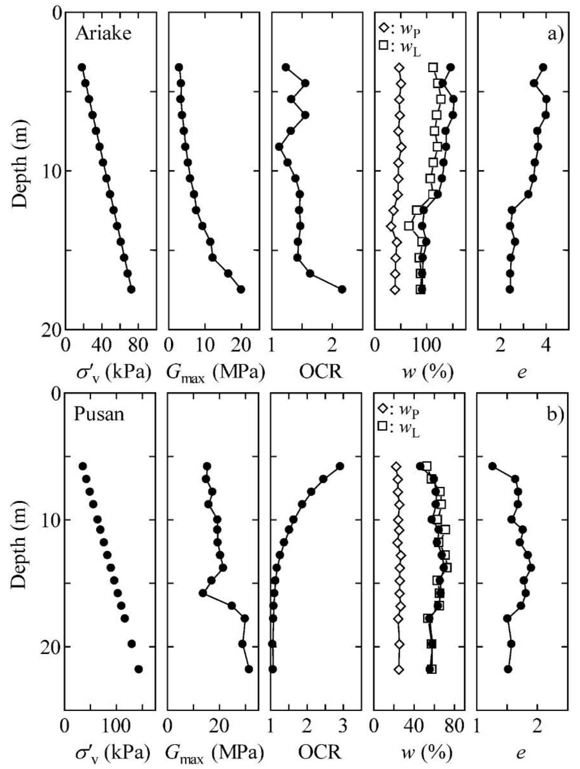

Fig. 4. Examples of geotechnical properties for tested sites (a: Ariake, b: Pusan)

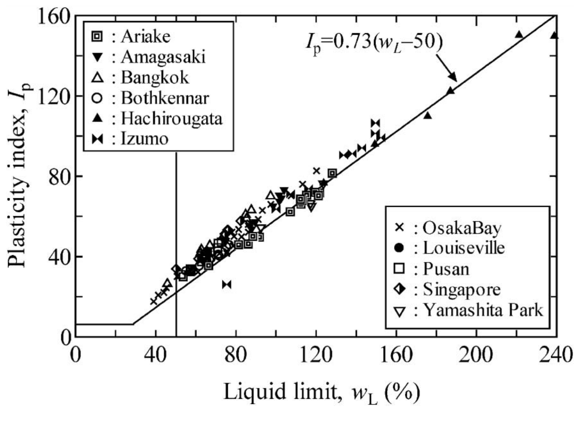

Fig. 5. Plasticity chart of the investigated sites

the effects of the K ratio on $(E_v)_u$ (or G_{vh}) are very small.

Elastic Modulus in Terms of e *and* p'

Figure 7 shows relationships among e, p' and $(E_v)_u$ for all tests (Note that specimens were consolidated under various K ratios) whose conditions are indicated in Table 2. As seen in Fig. 7, there exists a unique linear relationship between e and log $(E_v)_u$ for both NC and OC states, although its slope is different for NC and OC states. Figure 8 shows the relationship among e, p' and $(E_v)_u$ (or $3G_{vh}$) measured by the OEBE test for reconstituted Drammen clay and TX test for reconstituted Fujinomori clay. It can be also seen that the relationship between e and $(E_v)_u$ (or $3G_{vh}$) in semi-logarithmic scale is clearly linear

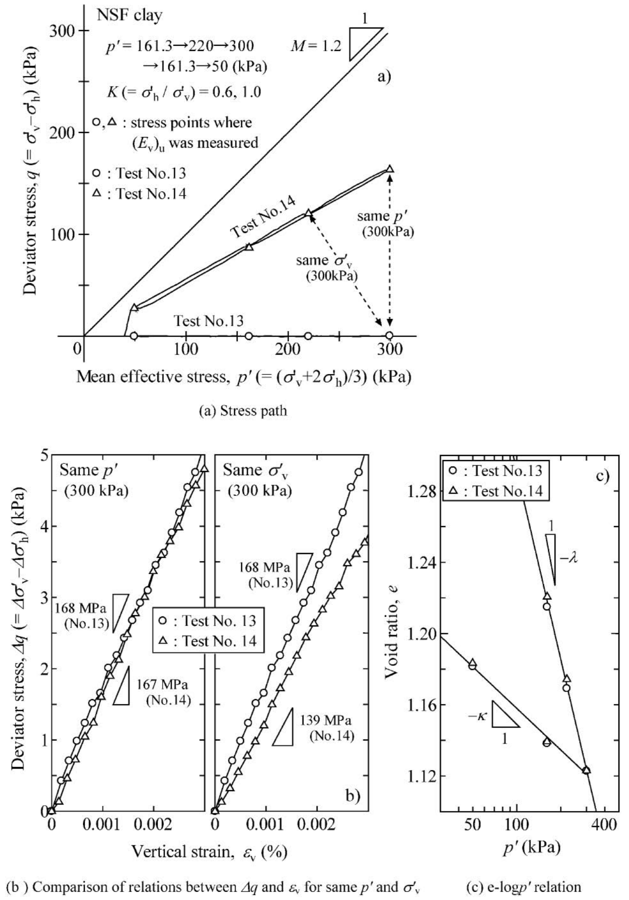

Fig. 6. Results of tests 13 and 14

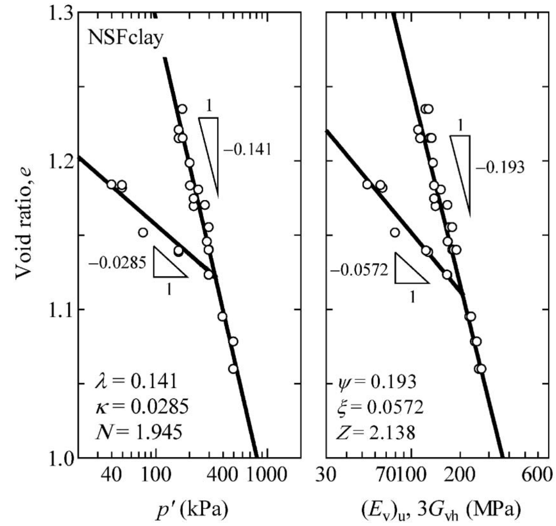

Fig. 7. Relationship among e, p' and $(E_v)_u$ for NSF clay

for these reconstituted clays.

Taking account of these experimental results and similar linearity in the relationship of e-log p', the $(E_v)_u$ can be expressed in the following forms for NC and OC states (Kawaguchi et al., 1999):

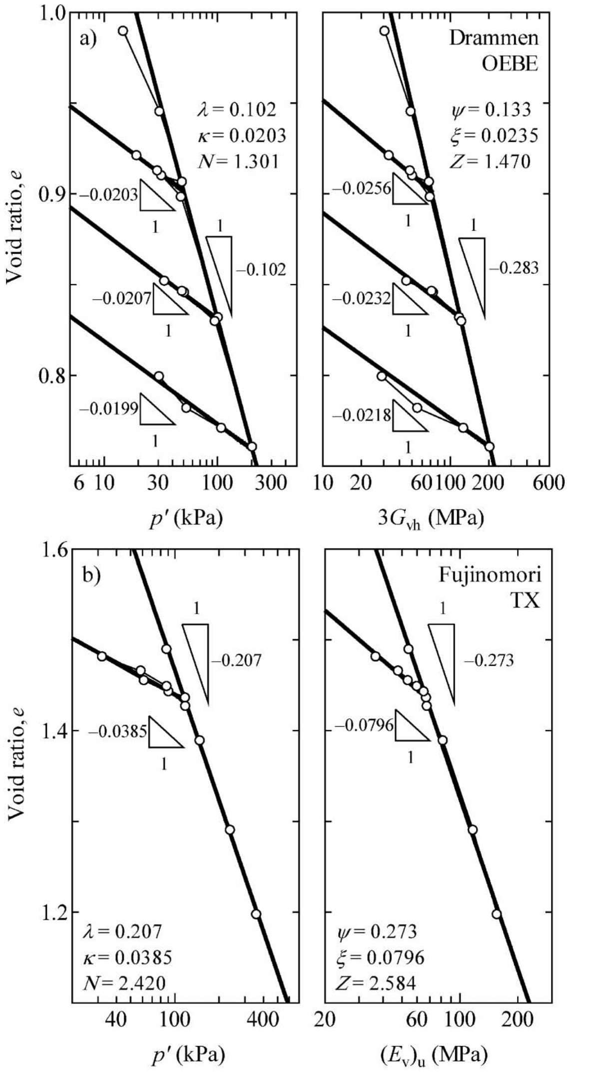

Fig. 8. Example showing the relationship among e, p' and $(E_v)_u$ (or $3G_{vh}$) (a: Drammen, b: Fujinomori)

$$(E_v)_u = \exp\left(\frac{Z-N}{\psi}\right) \cdot p'^{\frac{\lambda}{\psi}} \qquad \text{(NC)} \qquad (6a)$$

$$(E_v)_u = \exp\left(\frac{Z-N}{\psi}\right) \cdot p'^{\frac{\kappa}{\xi}} \cdot p'^{\frac{\lambda}{\psi}-\frac{\kappa}{\xi}}_{\max} \qquad \text{(OC)} \qquad (6b)$$

where, λ and κ are the slopes of the e–ln p' relationship at NC and OC states, respectively. In the same way, ψ, and ξ are the slopes of the e–ln $(E_v)_u$ relationship at NC and OC states, respectively. N and Z are the void ratios obtained by extrapolating at $p' = 1$ kPa and at $(E_v)_u = 1$ kPa, respectively. These experimental parameters obtained from reconstituted soils in this study are given in Table 1.

Relations between $(E_v)_u$ (or $3G_{vh}$) and p' are calculated by Eqs. (6a) and (6b); they are plotted in Fig. 9, where the tested values in Table 2 are also indicated. It should be kept in mind that the relation between $(E_v)_u$ and p' is very similar to that between undrained shear strength, s_u, and p': i.e., within certain stress levels, $(E_v)_u$ apparently increases linearly with p'. It is also interesting to note that the effect of OCR on $(E_v)_u$ is not so strong.

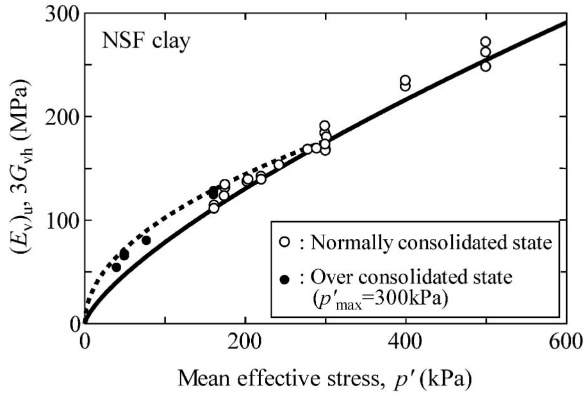

Fig. 9. A comparison of $(E_v)_u$ (or $3G_{vh}$) between the observed values and the calculated values using Eqs. (6a) and (6b) for all the tests shown in Fig. 7

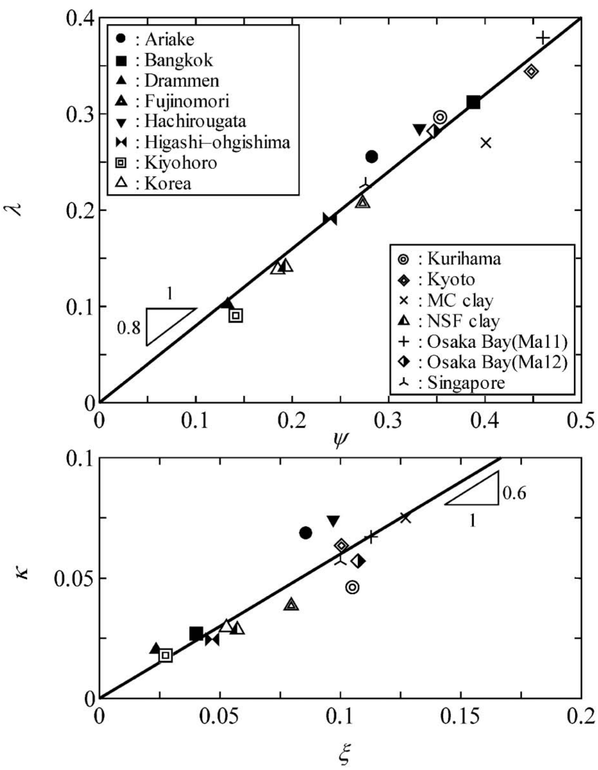

Fig. 10. Relationships between λ and ψ, and between κ and ξ

Interrelation among Parameters in Eq. (6)

Equations (6a) and (6b) proposed by Kawaguchi et al. (1999) require total six experimental parameters, i.e., λ, κ, ψ, ξ, Z and N, so that this equation can hardly be used in practice. Using six experimental parameters measured in this study (*see* in Table 1), it was tried to find interrelations among these parameters and correlate them to more fundamental geotechnical properties such as index properties. Linear relations between λ and ψ, as well as between κ and ξ are identified in Fig. 10, demonstrating that λ and κ can be correlated with ψ and ξ, respectively, as given by the following equations:

$$\lambda = 0.8 \cdot \psi \tag{7}$$
$$\kappa = 0.6 \cdot \xi \tag{8}$$

Furthermore, trials were made to correlate the term of $\exp\{(Z-N)/\psi\}$ in Eqs. (6a) and (6b) with fundamental parameters such as e, I_p and w_L. Among them, it is found that w_L can be correlated well with $\exp\{(Z-N)/\psi\}$, as seen in Fig. 11, except for three clays: Kiyohoro, Osaka Bay (Ma11) and Singapore clays. As can be seen in Table 1, I_p for Kiyohoro clay is relatively small, indicating that they contain a lot of silt or sand. Therefore, it may be anticipated that accuracy in measuring w_L would be poor. However, reasons for disagreements in Ma11 and Singapore clays are not identified. Ignoring these three clays, the term of $\exp\{(Z-N)/\psi\}$ can be expressed by Eq. (9):

$$\exp\left(\frac{Z-\mathrm{N}}{\psi}\right) = 60000 \cdot w_L^{-0.8} \tag{9}$$

Finally, $(E_v)_u$ or G_{max} is simply formulated by:

$$(E_v)_u = 60000 \cdot w_L^{-0.8} \cdot p'^{0.6} \cdot p'^{0.2}_{max} \tag{10}$$
$$G_{max} = 20000 \cdot w_L^{-0.8} \cdot p'^{0.6} \cdot p'^{0.2}_{max} \tag{2}$$

Instead of p'_{max}, if overconsolidation ratio is defined in terms of p', such as $(\mathrm{OCR})_{p'} = p'_{max}/p'$, then Eq. (2) becomes Eq. (11).

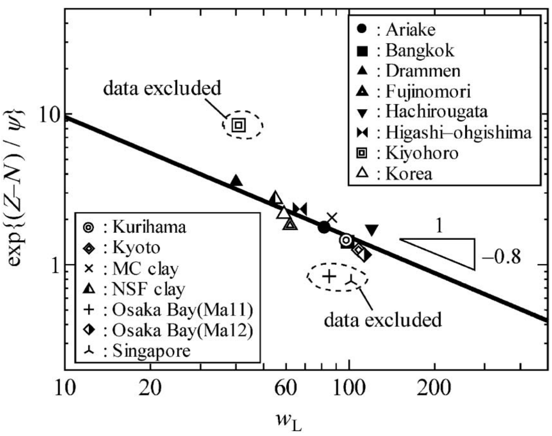

Fig. 11. Relationship between $\exp\{(Z\text{-}N)/\psi\}$ and w_L

$$G_{max} = 20000 \cdot w_L^{-0.8} \cdot (\mathrm{OCR})_{p'}^{0.2} \cdot p'^{0.8} \tag{11}$$

Viggiani and Atkinson (1995) also proposed the following equation for G_{max} measured from reconstituted soils.

$$\frac{G_{max}}{p'_r} = B \cdot \left(\frac{p'}{p'_r}\right)^n \cdot R_0^m \tag{12}$$

where, B, n and m are experimental parameters. In their paper, the coefficient of B was originally ''A'', but ''A'' has been used in this paper as in Eq. (1) so as to avoid confusion, ''B'' will be used in this paper. R_0 is OCR defined by p', being the same as $(\mathrm{OCR})_{p'}$ in Eq. (11). They tried these parameters to relate to plasticity index, I_p, as shown in Fig. 12. It is interesting to note that n and m in their tests are nearly constant for I_p and about 0.8 and 0.25, respectively. These values are very close to those measured in the present study, i.e., 0.8 and 0.2. Also it should be kept in mind that I_p is strongly related to w_L (*see* plastic chart, for example, Fig. 1). The trend that the B coefficient in Eq. (12) increases with the decrease in I_p is very similar to that of $w_L^{-0.8}$ in Eq. (11) or (2).

APPLICABILITY OF THE PROPOSED EQUATION TO G_{max} MEASURED IN THE FIELD

For application of the established Eq. (2) to the field, the current and the maximum mean effective stresses, p' and p'_{max} are required. In the field, however, these values are rarely available; especially the in-situ horizontal effective stress is unknown. Instead, the in-situ effective overburden pressure, σ'_{v0}, is suitable in practical applications. In addition, to take account of effects of p'_{max}, the yield consolidation pressure in one dimensional consolidation, σ'_{vy}, will be used in the formulation. It is well known that σ'_{vy} for natural clays is definitely larger than σ'_{v0} even for normally consolidated clay due to ageing effects. The validity adopting σ'_{vy} instead of p'_{max} will be discussed later in more detail. The value of σ'_{vy} is measured by Constant Rate of Strain at 0.02%/min.

$$G_{max} = 20000 \cdot w_L^{-0.8} \cdot f(\mathrm{OCR}) \cdot \sigma'^{0.8}_{v0} \tag{3}$$

where, $f(\mathrm{OCR})$ is a function of OCR ($=\sigma'_{vy}/\sigma'_{v0}$) and expressed by Eq. (4).

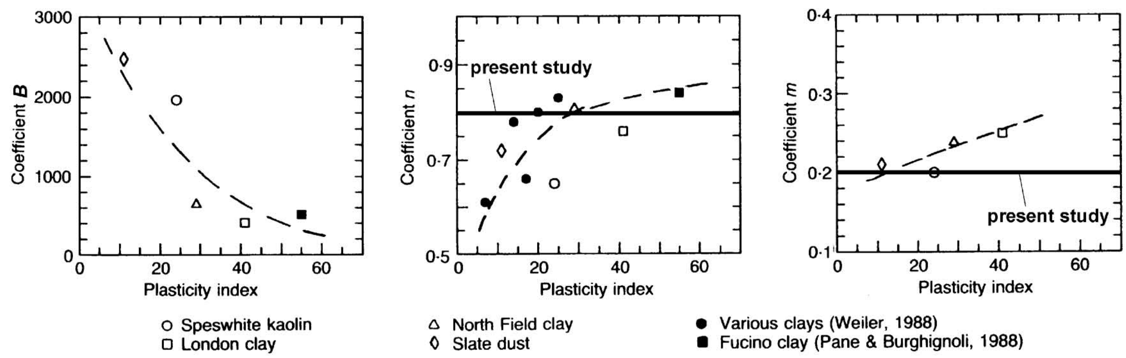

Fig. 12. Variation of stiffness parameter for G_{max} in Eq. (12) with plasticity index (after Viggiani and Atkinson, 1995, where lines from the present study are drawn)

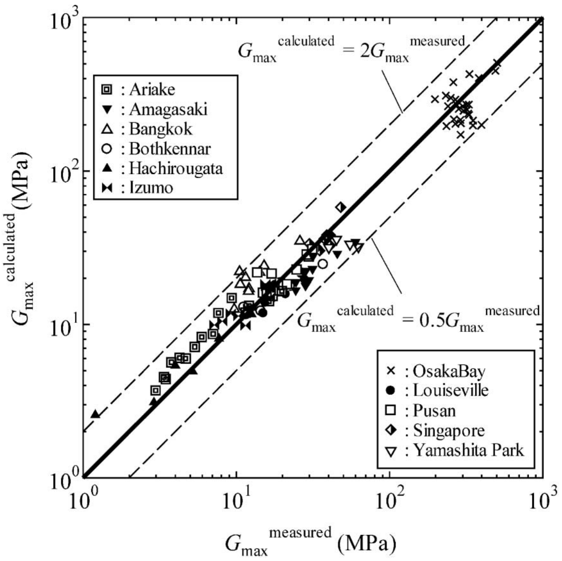

Fig. 13. Comparison between G_{max} calculated by Eq. (3) and G_{max} measured in the field

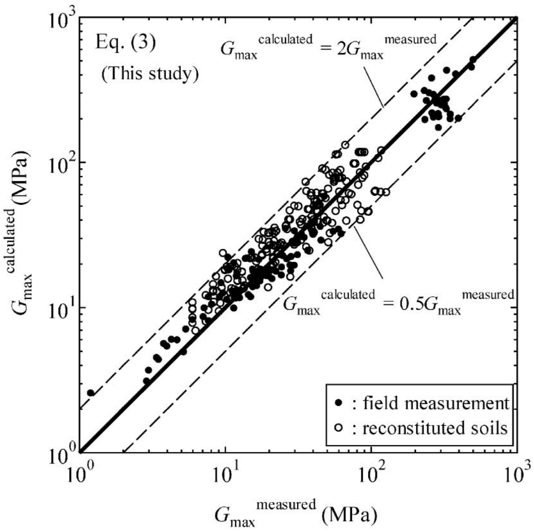

Fig. 14. Comparison between G_{max} calculated by Eq. (3) and G_{max} measured in the field and from reconstituted soils

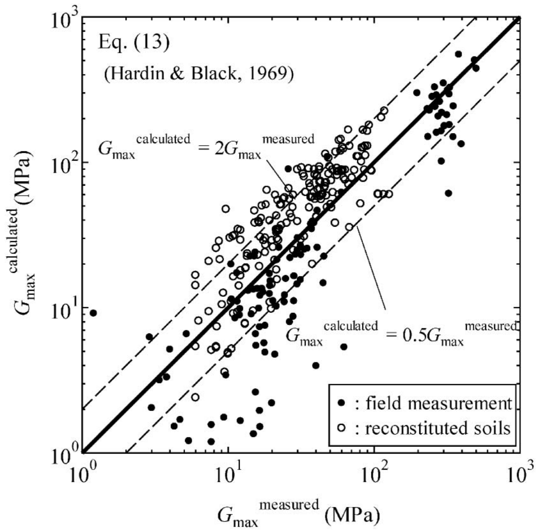

Fig. 15. Comparison between G_{max} calculated by Eq. (13) and G_{max} measured in the field and from reconstituted soils

$$f(\mathrm{OCR})=\left(\frac{2}{3}\,\mathrm{OCR}\right)^{0.2}\cdot\left(\frac{1+\mathrm{OCR}^{0.5}}{3}\right)^{0.6} \tag{4}$$

Detailed derivation of Eq. (4) may be referred in APPENDIX of this paper.

Comparison between G_{max} calculated by Eq. (3) ($G_{max}^{calculated}$) and G_{max} measured in the field ($G_{max}^{measured}$) is made in Fig. 13. Points distributed in the upper right of the figure are G_{max} measured at the construction site of the Kansai International Airport, where the site investigation was carried out at depths deeper than 300 m. Therefore, G_{max} itself is very large. It can be seen that almost all data are distributed in the range between 0.5 and 2.0 of $G_{max}^{measured}/G_{max}^{calculated}$. To reveal the superiority of Eq. (3), several well known equations are selected and their accuracies are compared.

$$G_{max}=3270\cdot\frac{(2.97-e)^2}{1+e}\cdot p'^{\,0.5}$$

(in kPa) (Hardin and Black, 1969) (13)

$$G_{max}=41600\cdot\left(0.67-\frac{e}{1+e}\right)\cdot\sigma_v'^{\,0.5}$$

(in kPa) (Shibata and Soelarno, 1978) (14)

$$G_{max}=5000\cdot e^{-1.5}\cdot\sigma_v'^{\,0.5}$$

(in kPa) (Shibuya and Tanaka, 1996) (15)

$$G_{max}(285-2\cdot I_p)\cdot p' \quad \text{(in kPa) (Zen et al., 1987)} \tag{16}$$

All equations except for Zen et al. (1987) are based on e and the exponent of effective stress (p' or σ_v') is 0.5. Also, in these equations, the coefficient corresponding to A in Eq. (1) is constant for any soil, i.e., not influenced by index properties. The term of OCR has disappeared in these equations, as has already been discussed. However, in the equation of Zen et al. (1987), G_{max} linearly increases with p' and A coefficient decreases with increase in I_p. This trend is the same as the equation proposed by the present study as well as Viggiani and Atkinson's equation, i.e., Eq. (12).

Results from the comparison are seen in Figs.14–18, where solid and open circles indicate G_{max} measured in the field and from reconstituted soils, respectively. As expected, a clear trend exists in G_{max} calculated from Eqs. (13)–(15) for the field measurement and laboratory testing from reconstituted soils. That is, most open circles (reconstituted soils) are located above the line indicating $G_{max}^{calculated}=G_{max}^{measured}$, while solid circles (measured in the field) are distributed below the line. In other words, Eqs. (13)–(15) tend to overestimate G_{max} for reconstituted soils, while they underestimate G_{max} measured in the field. As already discussed, the order of e in the field is always greater than that in reconstituted soil, even though p' and

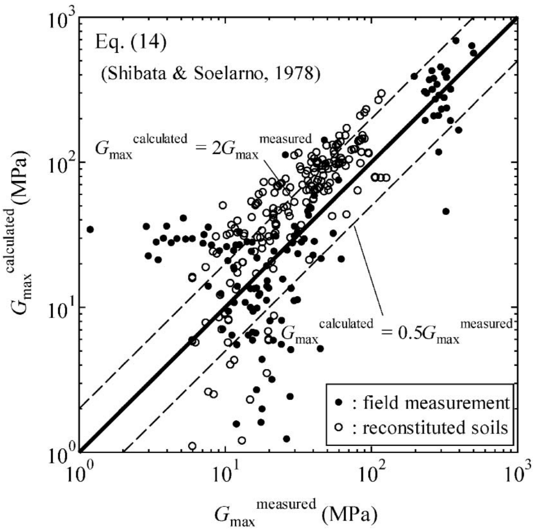

Fig. 16. Comparison between G_{max} calculated by Eq. (14) and G_{max} measured in the field and from reconstituted soils

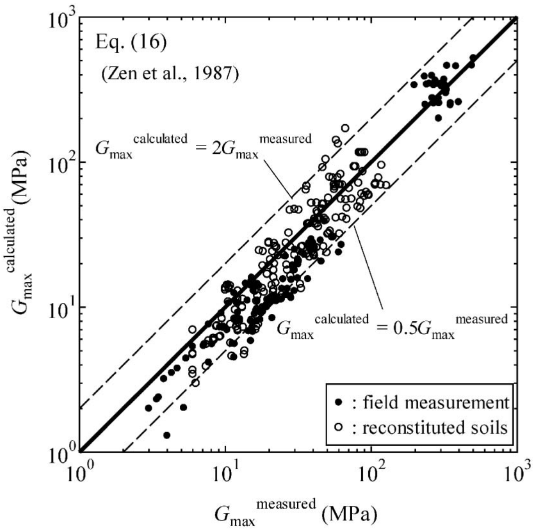

Fig. 18. Comparison between G_{max} calculated by Eq. (16) and G_{max} measured in the field and from reconstituted soils

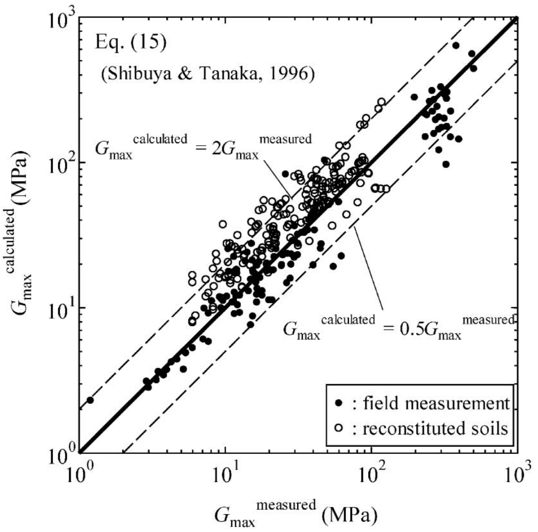

Fig. 17. Comparison between G_{max} calculated by Eq. (15) and G_{max} measured in the field and from reconstituted soils

OCR of reconstituted soils are the same as those in the field. Therefore, as far as based on e, it is impossible to formulate G_{max} equations valid for both measurements from field and laboratory tests using reconstituted soils. Contrary to these equations, Eq. (16) proposed by Zen et al. (1987) seems to be applicable to both reconstituted soils and field measurement, as seen in Fig. 18. It is interesting to note that even for greater G_{max} of the Osaka Pleistocene clays, Eq. (16) estimates G_{max} in the same order of accuracy as that by Eq. (3) proposed in this study, even though the exponent on p' is somewhat different between these equations. On the other hand, a slight difference between these two equations can be detected at smaller p': i.e., Zen et al.'s equation generally underestimates measured values.

In the proposed equation, the effect of σ'_{vy} on G_{max} is assumed to be the same as the maximum effective vertical stress in the past: i.e., σ'_{vmax}. However, it is well known that σ'_{vy} for naturally deposited clay, which is somewhat greater than σ'_{v0}, is not only created by the large consolidation pressure in the past, but also by ageing effects (*see*, for example, Bjerrum, 1967). In this sense, σ'_{vy} for natural deposits should be different from σ'_{vmax} for reconstituted soils, which have derived the Eq. (2). However, as indicated in Fig. 14, G_{max} for natural deposits can be simply correlated with σ'_{vy} in the same manner that G_{max} for reconstituted soil is related to σ'_{vmax}. This result can explain that the influence of the ageing effect on G_{max} can be simply considered as increase in σ'_{vy}.

CONCLUSIONS

Based on the laboratory tests such as bender element and cyclic/monotonic triaxial tests for various reconstituted soils, the shear modulus at small strain, G_{max}, can be simply formulated as:

$$G_{max} = 20000 \cdot w_L^{-0.8} \cdot p'^{0.6} \cdot p'^{0.2}_{max} \tag{2}$$

where, w_L is liquid limit in %, and p' and p'_{max} are the current mean effective stress at measurement of G_{max} and the maximum mean effective stress, respectively. Because this formulation is based on the mean effective stress, it is inconvenient to apply this equation to the field where the effective lateral pressure, σ'_h, is unknown, but the effective overburden pressure, σ'_{v0}, is only known. For this reason, Eq. (2) is transformed into Eq. (3) for its application to the field as:

$$G_{max} = 20000 \cdot w_L^{-0.8} \cdot f(\mathrm{OCR}) \cdot \sigma'^{0.8}_{v0} \tag{3}$$

where, f(OCR) is a function of OCR ($= \sigma'_{vy}/\sigma'_v$, where σ'_{vy} is the yield consolidation pressure) and expressed by Eq. (4).

$$f(\mathrm{OCR}) = \left(\frac{2}{3}\,\mathrm{OCR}\right)^{0.2} \cdot \left(\frac{1+\mathrm{OCR}^{0.5}}{3}\right)^{0.6} \tag{4}$$

The most important feature in Eqs. (2) and (3) is that they do not use the void ratio, e. Applicability of Eq. (3) was examined for the authors' data base. It is revealed that Eq. (3) can not only predict G_{max} for the reconstituted, but also G_{max} measured in the field. It is found that its accuracy lies in the range between 0.5 and 2.0 of $G_{max}^{measured}/G_{max}^{calculated}$. Most existing proposed equations overestimate G_{max} for reconstituted soils and underestimate G_{max} measured in the field, since they are based on e.

REFERENCES

1) Atkinson, J. H. (1975): Anisotropic elastic deformation in laboratory tests on undisturbed London Clay, *Géotechnique*, **25**, 357–374.
2) Bishop, A. W. and Hight, D. W. (1977): The value of Poisson's ratio in saturated soils and rocks stressed under undrained conditions, *Géotechnique*, **27**, 369–384.
3) Burland, J. B. (1990): On the compressibility and shear strength of natural clays, *Géotechnique*, **40**, 329–347.
4) Graham, J. and Houlsby, G. T. (1983): Anisotropic elasticity of a natural clay, *Géotechnique*, **33**, 165–180.
5) Hardin, B. O. and Black, W. L. (1969): Vibration modulus of normally consolidated clay, *ASCE*, **95**(SM6), 1531–1537.
6) Hwang, S. C. (1998): Study on deformation characteristics at small strains and evaluation of undrained shear strength of natural sedimentary clays, *DEng Thesis*, Graduate School of Engineering, Hokkaido University (in Japanese).
7) Jamiolkowski, M., Lancellotta, R. and Lo Presti, D. C. F. (1994): Remarks on the stiffness at small strains of six Italian clays, *Proc. Pre-failure Deformation of Geomaterials*, Balkema, **2**, 817–836.
8) Jovičić, V. and Coop, M. R. (1995): The measurement of stiffness anisotropy in clays with bender element tests in the triaxial apparatus, *ASTM*, **21**(1), 3–10.
9) Kawaguchi, T., Mitachi, T. and Shibuya, S. (1999): Quantifying deformation modulus of reconstituted clays at small strains, *JSCE*, (638/III-49), 179–191 (in Japanese).
10) Kawaguchi, T., Mitachi, T. and Shibuya, S. (2001): Evaluation of shear wave travel time in laboratory bender element test, *Proc. 15th ICSMGE*, **1**, 155–158.
11) Kawaguchi, T., Mitachi, T., Shibuya, S. and Sano, Y. (2002): Development of an elaborate triaxial testing system for deformation of clay, *JSCE*, (708/III-59), 175–186 (in Japanese).
12) Kawaguchi, T., Mitachi, T., Shibuya, S. and Sato, S. (2003): Evaluation of deformation modulus of clay at small strains based on isotropic elasticity, *Proc. Deformation Characteristics of Geomaterials, IS-Lyon*, Balkema, **1**, 211–219.
13) Kawaguchi, T., Yamashita, S. and Shibuya, S. (2007): Inherent and stress-induced anisotropy of elastic shear modulus for soils, *Proc. 13th ARC on SMGE*, **1**, 15–18, Millpress.
14) Larsson, R. and Åhnberg, H. (2005): On the evaluation of undrained shear strength and preconsolidation pressure from common field tests in clay, *Can. Getech. J.*, **42**, 1221–1231.
15) Li, D. J. (2003): Study on structure and cementation effects of natural sedimentary clay, *DEng Thesis*, Graduate School of Engineering, Hokkaido University (in Japanese).
16) Lings, M. L., Pennington, D. S. and Nash, D. F. T. (2000): Anisotropic stiffness parameters and their measurement in a stiff natural clay, *Géotechnique*, **50**, 109–125.
17) Marcuson, III, W. F. and Wahls, H. E. (1972): Time effects on dynamic shear modulus of clays, *ASCE*, **98**(SM12), 1359–1373.
18) Nash, D. F. T., Powell, J. J. M. and Lloyd, I. M. (1992): Initial investigations of the soft clay test site at Bothkennar, *Géotechnique*, **42**, 163–181.
19) Shibata, T. and Soelarno, D. S. (1978): Stress-strain characteristics of clays under cyclic loading, *JSCE*, (276), 101–110.
20) Shibuya, S. and Tanaka, H. (1996): Estimate of elastic shear modulus in Holocene soil deposits, *Soils and Foundations*, **36**(4), 45–55.
21) Shibuya, S. and Mitachi, T. (1997): Development of a fully digitized triaxial apparatus for testing soils and soft rocks, *Geotechnical Engineering Journal*, **28**, 183–207.
22) Shibuya, S., Hwang, S. C. and Mitachi, T. (1997): Elastic shear modulus of soft clays from shear wave velocity measurement, *Géotechnique*, **47**, 593–601.
23) Tanaka, H., Tanaka, M., Iguchi, H. and Nishida, K. (1994): Shear modulus of soft clay measured by various kinds of tests, *Proc. International Symposium on Pre-failure Deformation Characteristics of Geomaterials*, **1**, 235–240.
24) Tanaka, H., Locat, J., Shibuya, S., Tan, T. S. and Shiwakoti, D. R. (2001a): Characterization of Singapore, Bangkok and Ariake clays, *Can. Getech. J.*, **38**, 378–400.
25) Tanaka, H., Shiwakoti, D. R., Mishima, O., Watabe, Y. and Tanaka, M. (2001b): Comparison of mechanical behavior of two overconsolidated clays: Yamashita and Louiseville clays, *Soils and Foundations*, **41**(4), 73–87.
26) Tanaka, H., Mishima, M., Tanaka, M., Park, S., Z., Jeong, G., H. and Locat, J. (2001c): Characterization of Yangsan clay, Pusan, Korea, *Soils and Foundations*, **41**(2), 89–104.
27) Tanaka, H. (2002): Re-examination of established relations between index properties and soil parameters, *Proc. Coastal Geotechnical Engineering in Practice*, **2**, 3–25.
28) Tanaka, H. (2002): A comparative study on geotechnical characteristics of marine soil deposits worldwide, *International Journal of Offshore and Polar Engineering*, **12**(2), 81–88.
29) Tanaka, H., Ritoh, F. and Omukai, N. (2002): Sample quality retrieved from great depth and its influence on consolidation properties, *Can. Geotech. J.* (in press).
30) Tanaka, H., Kang, M. S. and Watabe, Y. (2004): Ageing effects on consolidation properties -Based on the site investigation of Osaka Pleistocene clays, *Soils and Foundations*, **44**(6), 39–52.
31) Tanaka, H. (2006): Geotechnical properties of Hachirogata clay, *The 2nd Characterization and Engineering Properties of Natural Soils* (in press).
32) Temma, M., Shibuya, S., Tanaka, H., Mishima O. and Tanaka, M. (2000): A case study on evaluating ageing effects on mechanical behavior of over-consolidated clay ground, *Symposium on Overconsolidated Soils and Mechanical Behavior of Overcosolidated Ground*, JGS, 111–116 (in Japanese).
33) Viggiani, G. and Atkinson, J. H. (1995): Stiffness of fine-grained soil at very small strains, *Géotechnique*, **45**(2), 249–265.
34) Yamashita, S. and Suzuki, T. (2001): Small strain stiffness on anisotropic consolidated state of sands by bender elements and cyclic loading tests, *Proc. 15th ICSMGE*, **1**, 325–328.
35) Yimsiri, S. and Soga, K. (2002): Application of micromechanics model to study anisotropy of soils at small strains, *Soils and Foundations*, **42**(5), 15–26.
36) Yimsiri, S. and Soga, K. (2003): Small-strain stiffness anisotropy: relationship between continuum model and micromechanics model, *Deformation Characteristics of Geomaterials, IS-Lyon*, **1**, 313–319, Balkema.
37) Zen, K., Umehara, Y. and Hamada, K. (1978): Laboratory tests ind in situ seismic survey on vibratory sher modulus of clayey soils with various plasticities, *Proc. 5th Japan Earthquake Engineering Symposium*, 721–728.
38) Zen, K., Yamazaki, H. and Umehara, Y. (1987): Experimental study on shear modulus and damping ratio of natural deposits for seismic response analysis, *Report of the Port and Harbour Research Institute*, **26**(1), 41–113.

APPENDIX: DERIVATION OF FUNCTION OF *f*(OCR)

Using of $(\mathrm{OCR})_{p'}$ defined by Eqs. (A1) and (2) can be expressed by Eq. (A2) (i.e., Eqs. (3) and (11)).

$$(\mathrm{OCR})_{p'}=\frac{p'_{max}}{p'}=\frac{\sigma'_{vy}+2\sigma'_{hy}}{\sigma'_{v0}+2\sigma'_{h0}} \tag{A1}$$

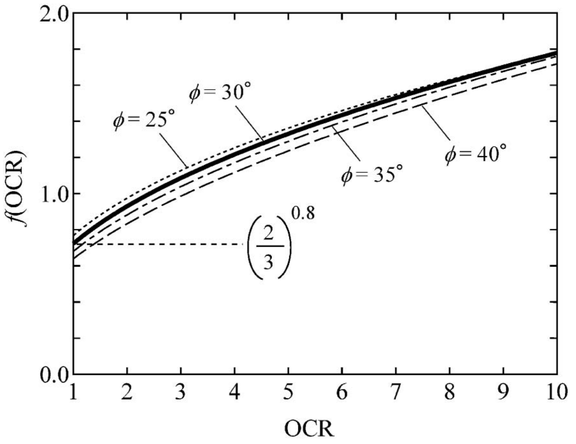

Fig. A1. Relationship between *f*(OCR) and OCR

$$\begin{aligned} G_{max} &= 20000 \cdot w_L^{-0.8} \cdot p'^{0.2}_{max} \cdot p'^{0.6} \\ &= 20000 \cdot w_L^{-0.8} \cdot (\mathrm{OCR})_{p'}^{0.2} \cdot p'^{0.8} \\ &= 20000 \cdot w_L^{-0.8} \cdot f(\mathrm{OCR}) \cdot \sigma'^{0.8}_{v0} \end{aligned} \tag{A2}$$

It is well known that the coefficient of earth pressure at rest for NC clay, $K_{0(NC)}$, and K_0 for OC clay, $K_{0(OC)}$ are experimentally formulated by following equations:

$$K_{0(NC)} = 1 - \sin\phi' = \frac{\sigma'_{hy}}{\sigma'_{vy}} \tag{A3}$$

$$K_{0(OC)} = K_{0(NC)} \cdot \mathrm{OCR}^{\sin\phi'} = \frac{\sigma'_{h0}}{\sigma'_{v0}} \left(\mathrm{OCR} = \frac{\sigma'_{vy}}{\sigma'_{v0}}\right) \tag{A4}$$

From Eq. (A2), $f(\mathrm{OCR})$ is:

$$\begin{aligned} f(\mathrm{OCR}) &= (\mathrm{OCR})_{p'}^{0.2} \cdot \left(\frac{p'}{\sigma'_{v0}}\right)^{0.8} \\ &= \left\{\frac{\mathrm{OCR} + 2\mathrm{OCR}(1-\sin\phi')}{1 + 2(1-\sin\phi') \cdot \mathrm{OCR}^{\sin\phi'}}\right\}^{0.2} \\ &\quad \times \left\{\frac{1 + 2(1-\sin\phi) \cdot \mathrm{OCR}^{\sin\phi}}{3}\right\}^{0.8} \end{aligned} \tag{A5}$$

As shown in Eq. (A5), $f(\mathrm{OCR})$ is not only a fucntion of OCR, but also $\sin\phi'$. However, as shown in Fig. A1, the influence of ϕ' is very small, and the difference caused by assumption of $\sin\phi' = 0.5$ can be ignored. Therefore, $f(\mathrm{OCR})$ is simply given in Eq. (4).

$$f(\mathrm{OCR}) = \left(\frac{2}{3}\mathrm{OCR}\right)^{0.2} \cdot \left(\frac{1 + \mathrm{OCR}^{0.5}}{3}\right)^{0.6} \tag{4}$$